Journal of Luminescence 137 (2013) 59–63

Contents lists available at SciVerse ScienceDirect

Journal of Luminescence

journal homepage: www.elsevier.com/locate/jlumin

Hybrid white organic light-emitting diodes with improved color stability and negligible efficiency roll-off based on blue fluorescence and yellow phosphorescence

Xuehui Wang [a,1], Shiming Zhang [a,b,1], Ziyang Liu [a], Shouzhen Yue [a], Zhensong Zhang [a], Yu Chen [a], Guohua Xie [c], Qin Xue [d], Yi Zhao [a,*], Shiyong Liu [a]

[a] State Key laboratory on Integrated Optoelectronics, College of Electronic Science and Engineering, Jilin University, Changchun 130012, People's Republic of China
[b] Département of Chemical Engineering, École Polytechnique de Montréal, Montréal, Québec, Canada H3C3J7
[c] Institut für Angewandte Photophysik, Technische Universtität Dresden, 01062 Dresden, Germany
[d] College of Physical Science and Technology, Central China Normal University, Wuhan 430079, People's Republic of China

ARTICLE INFO

Article history:
Received 13 September 2012
Received in revised form
16 November 2012
Accepted 21 December 2012
Available online 28 December 2012

Keywords:
Hybrid WOLED
Interlayer
DSA-Ph
PO-01
High stability

ABSTRACT

We report hybrid white organic light-emitting diodes (WOLEDs) based on yellow phosphorescence of Iridium (III) bis(4-phenylthieno[3, 2-*c*]pyridinato-*N*, $C^{2'}$)acetylacetonate (PO-01) and blue fluorescence of *p*-bis (*p*-*N*,*N*-diphenyl-amino-styryl) benzene (DSA-Ph). By introducing appropriate thickness of tris (phenylpyrazole) Iridium [$Ir(ppz)_3$] as interlayer between the adjacent emission layers, taking advantage of the assistance electron-transporting behavior of guest molecules, efficient WOLEDs with negligible efficiency roll-off and high color stability are obtained. The best device shows a peak current efficiency of 21.0 cd/A at 2, 300 cd/m^2 and the value can be maintained as high as 20.1 cd/A at 9, 300 cd/m^2. Furthermore, the Commission Internationale de L'Eclairage coordinate of the corresponding device only changes marginally from (0.41, 0.46) to (0.40, 0.46) over 10^3–10^4 cd/m^2.

1. Introduction

White organic light-emitting diodes (WOLEDs) have drawn tremendous attention and are expected to dominate the next-generation flat-panel display and solid-state lighting due to their merits of ultra-thin, light weight, and environmental friendliness [1,2]. In terms of materials, nowadays, phosphorescent material is extensively adopted to obtain high efficiency OLEDs due to its potential for achieving 100% internal quantum efficiency [3]. However, up to now, high efficiency blue phosphor with acceptable operational lifetime still has not been developed, which limits the developing of all-phosphor OLEDs [4]. In recent years, WOLEDs which combine blue fluorescent with red (or yellow) phosphorescent emitters (hybrid WOLED) have been designed [5], and the hybrid WOLEDs can indeed show improved operational stability [6]. In addition, for practical lighting purpose, WOLEDs also need to offer high efficiency as well as stable performance over a wide working-luminance range [7–9]. Therefore, the study of high efficiency hybrid WOLEDs with excellent stability is indispensable.

In this paper, we fabricated hybrid WOLEDs using yellow phosphorescence Iridium (III) bis(4-phenylthieno[3,2-*c*]pyridinato-*N*, $C^{2'}$)acetylacetonate (PO-01) and blue fluorescence 2-methyl-9,10-di (2-naphthyl) anthracene (MADN): *p*-bis (*p*-*N*,*N*-diphenyl-amino-styryl) benzene (DSA-Ph) based on different device architectures. By introducing appropriate thickness of tris (phenylpyrazole) Iridium [$Ir(ppz)_3$] as interlayer between the adjacent blue emission layer (B-EML) and yellow EML (Y-EML), utilizing DSA-Ph as well as PO-01 molecules as assistance electron-transporting channels, devices with negligible efficiency roll-off and high color stability are achieved. The best device shows a peak current efficiency (CE) of 21.0 cd/A at 2, 300 cd/m^2 and the value can be maintained as high as 20.1 cd/A at 9, 300 cd/m^2, besides, the Commission Internationale de L'Eclairage (CIE) coordinate of the corresponding device only changes marginally from (0.41, 0.46) to (0.40, 0.46) over 10^3–10^4 cd/m^2.

2. Experimental details

The glass coated with a layer of indium tin oxide (ITO) with a sheet resistance of 20 Ω/square was adopted as the substrate for OLEDs. Prior to film deposition, the substrates were cleaned by scrubbing and sonication, and then treated with oxygen plasma for 10 min to enhance the surface work function of ITO anode. All organic layers were deposited under high vacuum ($<4\times10^{-6}$ Torr). 4,4,4-tris(3-methylphenylphenylamino)-triphenylamine (*m*-MTDATA) and

* Corresponding author. Tel.: +86 431 85168242 8301; fax: +86 431 85168270.
E-mail address: yizhao@jlu.edu.cn (Y. Zhao).
[1] These authors contributed equally to this work.

0022-2313/$ - see front matter © 2012 Elsevier B.V. All rights reserved.
http://dx.doi.org/10.1016/j.jlumin.2012.12.031

7-diphenyl-1,10-phenanthroline (BPhen), serve as hole-transporting layer (HTL), and electron-transporting layer (ETL), respectively. $Ir(ppz)_3$ was served as interlayer, 4, 4-*N*,*N*-dicarbazole-biphenyl (CBP) served as the host for PO-01. After deposition of LiF, the samples were transferred to metal chamber, which resulted in a vacuum break due to the change of the shadow masks to determine the active area. The thermal deposition rates were 0.1, 0.05, and 0.5 nm/s for organic materials, LiF, and Al, respectively. The thicknesses of these deposited layers and the evaporation rate of individual material were monitored in situ using an oscillating quartz thickness monitor. The active area of the device was 4 mm^2. Molecular structural formulas of some of the materials used in the OLEDs are shown in Scheme 1. The electroluminescent (EL) spectra and CIE coordinates of the devices were measured by a PR650 spectroscan spectrometer, and the current (*J*)–voltage (*V*)-luminance characteristics were recorded simultaneously by combining the spectrometer with Keithley model 2400 programmable voltage–current source. The efficiency calculation method the device is the same as S.R. Forrest's group by assuming the emissive profiles of the device as the Lambertian emitter's [10]. All measurements were carried out at room temperature under ambient conditions.

3. Results and discussions

We first demonstrated two sets of devices as follows and the corresponding configurations are shown in Fig. 1(a) and (b).

A-series: ITO/*m*-MTDATA (45 nm)/$Ir(ppz)_3$ (10 nm)/CBP: PO-01 (10 nm, *6* wt%)/MADN: DSA-Ph (*x* nm, *5* wt%)/BPhen (50 nm)/LiF (1 nm)/Al (100 nm), $x=10$, 15, 20 and 25 for devices A_1, A_2, A_3 and A_4, respectively.

B-series: ITO/*m*-MTDATA (45 nm)/$Ir(ppz)_3$ (10 nm)/MADN: DSA-Ph (*x* nm, *5* wt%)/CBP: PO-01 (5 nm, *6* wt%)/MADN: DSA-Ph (10-*x* nm, *5* wt%)/BPhen (50 nm)/LiF (1 nm)/Al (100 nm), $x=2$, 3, 4 and 5 for devices B_1, B_2, B_3 and B_4, respectively.

The normalized EL spectra of A-series devices at different applied voltages are illustrated in Fig. 2. We can see all devices show a PO-01 dominated EL emission. Besides, interestingly, despite the B-EML thickness increases from A_1 to A_4, the blue emission with respect to yellow emission (ratio of the photons from DSA-Ph and PO-01: $R_{B/Y}$) was observed to decrease contrarily. In order to reveal the reason for this unusual phenomenon, electron-only and hole-only devices were fabricated and tested as shown in Fig. 3. We can see from Fig. 3 that an obvious increase in electron mobility can be observed upon doping DSA-Ph into MADN, which indicates that DSA-Ph serves as a transporting-channel for electrons, whereas DSA-Ph in MADN has almost no influence on hole-transporting. Hence, the increase in B-EML will prevent more holes from transporting to the B-EML/BPhen interface than electrons to the Y-EML/$Ir(ppz)_3$ interface. In this case, more holes will be used for PO-01 emission, resulting in a decrease in the $R_{B/Y}$ value inevitably.

Fig. 4(a) and (b) shows the CE versus luminance curves of devices A and B. Unfortunately, although B-series devices emit better white color, they exhibit a rather low CE value compared with A-series.

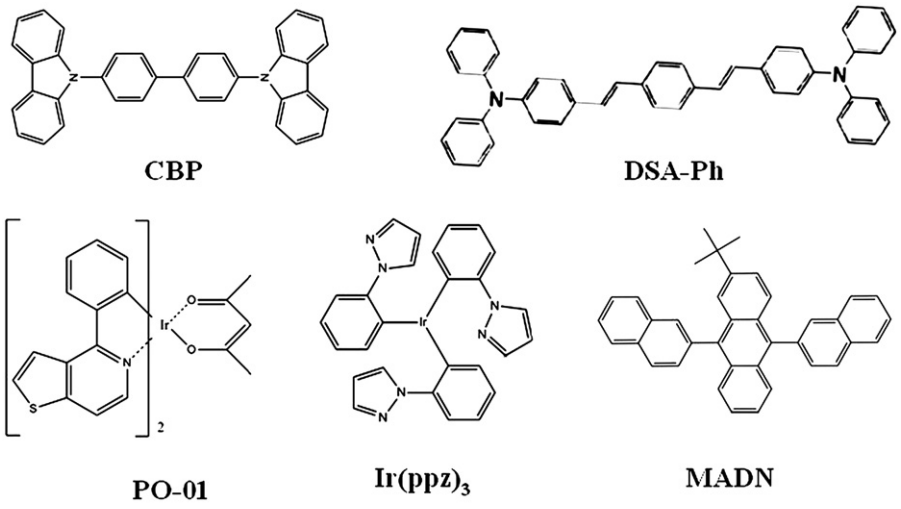

Scheme 1. Molecular structures of some materials used in this study.

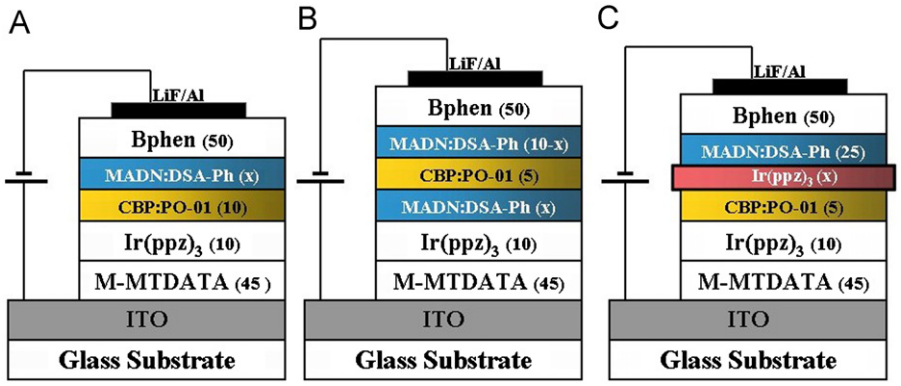

Fig. 1. Schematic layer stack of the investigated OLEDs.

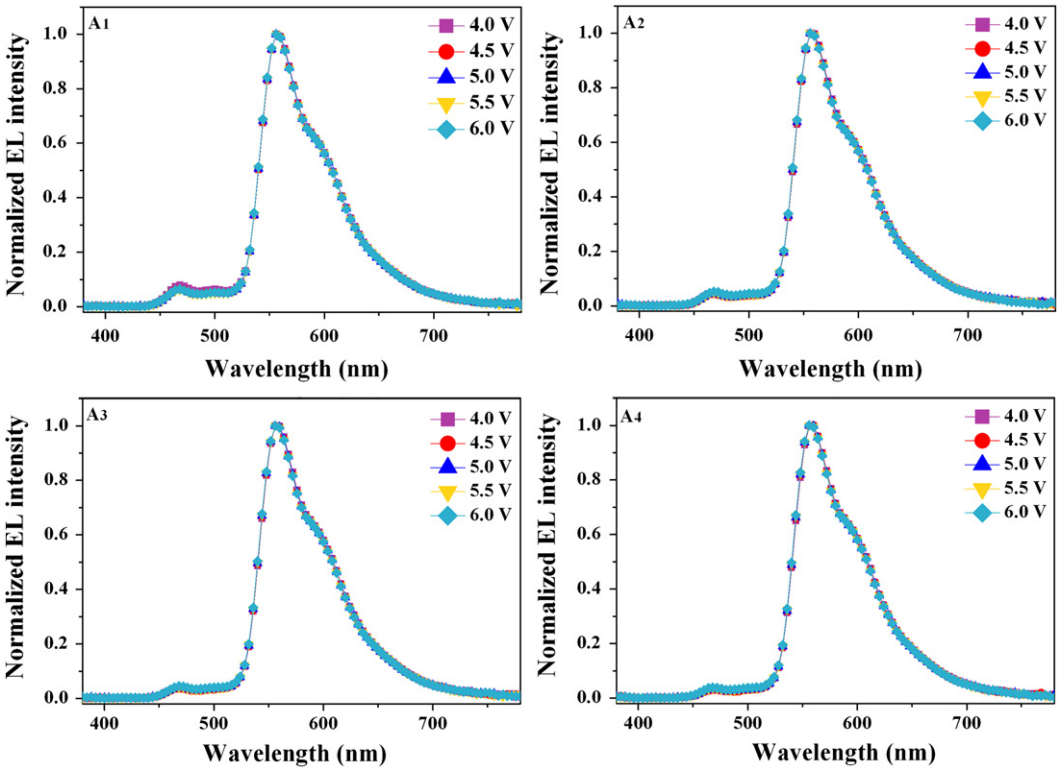

Fig. 2. Normalized EL spectra of A-series devices at different applied voltages.

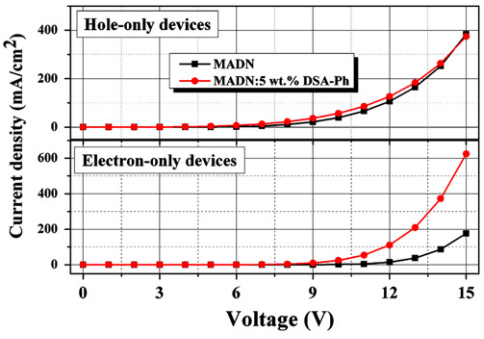

Fig. 3. *J–V* characteristics of the hole-only devices: ITO/MoO*x* (10 nm)/*m*-MTDATA (40 nm)/Ir(ppz)$_3$ (10 nm)/*X* (30 nm)/Ir(ppz)$_3$ (10 nm)/*m*-MTDATA (40 nm)/MoO*x* (10 nm)/Al (100 nm), and electron-only devices: ITO/LiF(1 nm)/Bphen (40 nm)/*X* (30 nm)/Bphen (40 nm)/LiF (1 nm)/Al (100 nm). Here *X* are MADN and 5 wt% DSA-Ph doped MADN, respectively.

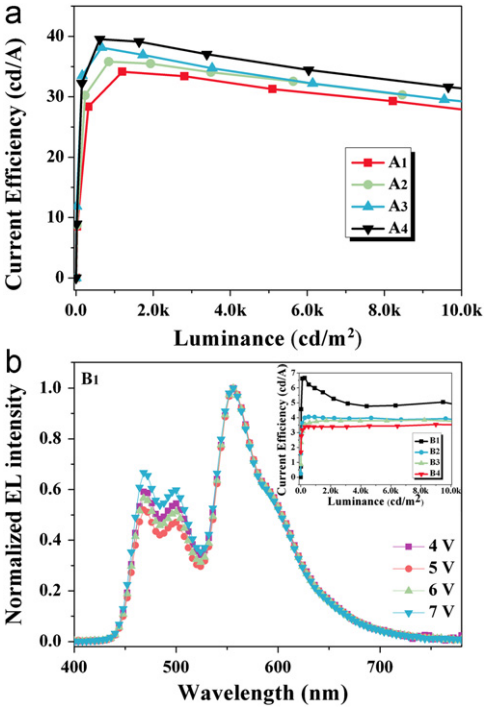

Fig. 4. (a) Luminance-CE curves of A-series devices; (b) normalized EL spectra of device B_1. Inset: luminance-CE curves of B-series devices.

We afterwards further analyzed the lowest unoccupied molecular orbital (LUMO) and highest occupied molecular orbital (HOMO) energy levels as well as the triplet energy levels of the materials [11–13] (shown in Fig. 5) and attributed the results to the severe triplet energy loss in the B-EML. Depicted in Fig. 5 (lower), the triplet energy level of Ir(ppz)$_3$ and CBP are both higher than that of DSA-Ph, hence, the triplet excitons formed in these adjacent two layers tend to diffuse into the B-EML with lower triplet level (processes ① and ②), following a downward energy transfer and non-radiative decay of triplets in fluorescence DSA-Ph, which accounts for the performance deterioration in B-series devices.

In the view of above considerations, we, in succession, demonstrated another C-series devices based on A-series device architecture. In the C-series devices, an thin Ir(ppz)$_3$ interlayer was introduced between the B-EML and the Y-EML in order to build an exciton recombination zone for blue emission, the structure diagram is shown in Fig. 1(c).

C-series: ITO/*m*-MTDATA (45 nm)/Ir(ppz)$_3$ (10 nm)/CBP: PO-01 (5 nm, 6 wt%)/Ir(ppz)$_3$ (*x* nm)//MADN: DSA-Ph (25 nm, 5 wt%)/BPhen (50 nm)/LiF (1 nm)/Al (100 nm), $x=1$, 2, 3 and 4 for devices C_1, C_2, C_3 and C_4, respectively.

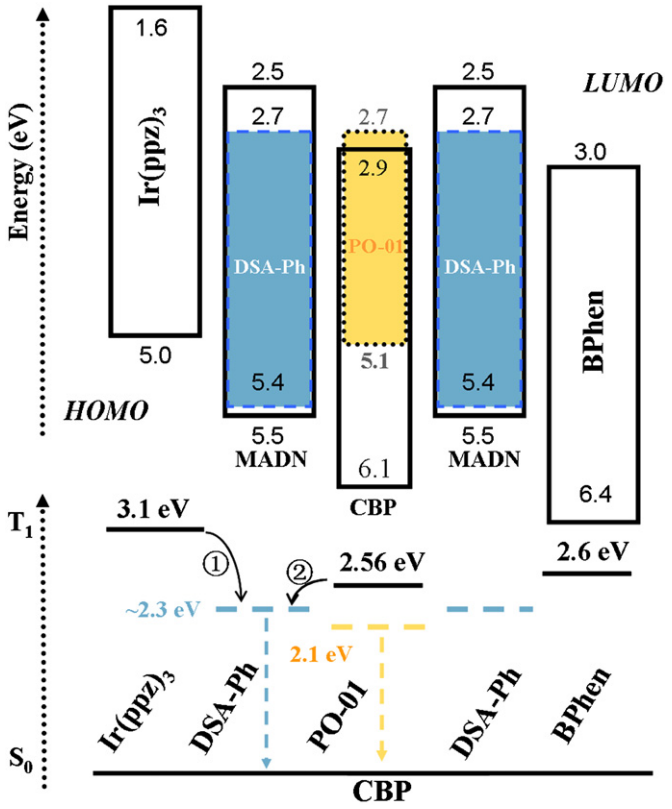

Fig. 5. Frontier HOMO-LUMO energy levels of C-series devices (upper) and triplet energy levels of the materials studied (lower).

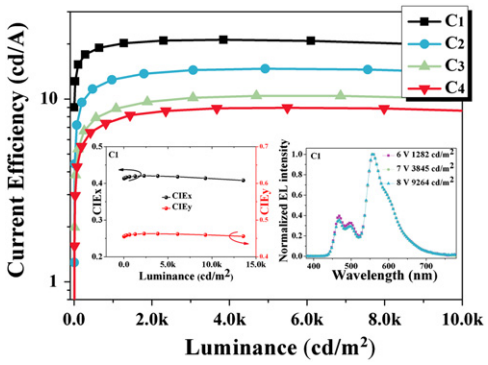

Fig. 6. Luminance-CE curves of C-series devices. The lower left-hand inset indicates the CIE coordinates variation versus luminance and normalized EL spectra of device C_1 over 10^3–10^4 cd/m^2 is shown in the lower right-hand inset.

The purpose of the Ir(ppz)$_3$ interlayer introduced herein is to function as a electron blocking layer to block electrons for the B-EML due to its inherent high LUMO level, thus, an increase in $R_{B/Y}$ value can be expected, which is crucial for obtaining a white-color device.

Fig. 6 provides a summary performance of C-series devices. We can see that device C_1 shows a balanced spectrum as expected and a peak CE of 21.0 cd/A at 2, 300 cd/m^2, the values can be maintained as high as 20.1 cd/A at 9, 300 cd/m^2. More significantly, the corresponding CIE coordinate only changes marginally from (0.41, 0.46) to (0.40, 0.46) over 10^3–10^4 cd/m^2. The stability both in efficiency and CIE coordinate of device C_1 is comparable with some of the high performance WOLEDs reported in

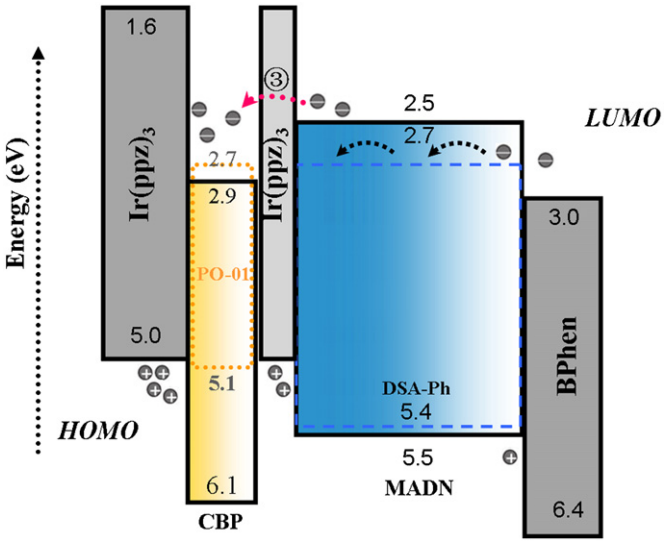

Fig. 7. Schematic of the processes taking place in the EML during voltage application.

literatures so far [6,14–17]. We ascribe the results to efficient electron-transporting into the EMLs. As is known, electrons are normally minor carriers compared with holes within an OLED, and their equilibrium distribution plays a crucial role in obtaining a device with highly stable performance. As shown in Fig. 7, even at a lower applied voltage, electrons can be easily transported to the B-EML/Ir(ppz)$_3$ interface (blue recombination zone) due to the assistance of DSA-Ph molecular as mentioned above. Once arriving at the interface, a fraction of electrons will form excitons with the holes confined within the Ir(ppz)$_3$ interlayer, whereas the rest can pass the 1-nm interlayer via tunneling behavior [18] (process ③) and then rapidly reach the Y-EML/Ir(ppz)$_3$ interface to harvest yellow color because doping PO-01 into CBP also exhibits improved electron mobility compared with pure CBP (the details will be published elsewhere). That is, stable electron distribution can be realized at relatively lower applied voltages via sequential assistance electron-transporting behavior of DSA-Ph and PO-01 molecules, which contributes to the high stability of device C_1.

The hybrid WOLED studied here can also be expected to have longer operation lifetime due to the excellent stability of blue fluorescence DSA-Ph [19]. The performances can be further optimized by adopting p–i–n structure to achieve more efficient carrier injection [20] and using a periodic outcoupling structure to increase the light extraction [21]. We anticipate seeing a more efficient WOLED based on this study in the future.

4. Conclusions

In summary, we have demonstrated hybrid WOLEDs using phosphorescence PO-01 and fluorescence DSA-Ph based on different structures. Detailed investigations are implemented to analysis the performance difference between the devices. By using Ir(ppz)$_3$ as interlayer and guest molecules as assistance electron-transporting channels, high color stability device with negligible efficiency roll-off is finally obtained after optimization. The corresponding device shows high CE of 21.0 cd/A at 2, 300 cd/m^2 and 20.1 cd/A at 9, 300 cd/m^2 with CIE coordinates change marginally from (0.41, 0.46) to (0.40, 0.46) over 10^3–10^4 cd/m^2. The high performance stability, which is essential for WOLEDs, makes the device have potential application in future practical solid-state lighting.

Acknowledgment

X.W. fabricated the devices; S.Z. designed the experiments and wrote the manuscript. All authors contributed to the discussion of the results. We would like to thank all the researchers who participated in this work and whose names appear in references. We also greatly acknowledge funding for this research from the National Key Basic Research and Development Program (973) of China under Grant no. 2010CB327701 and the National Natural Science Foundation of China (Grant nos. 60977024 and 61275033).

References

[1] B. D'Andrade, M. Thompson, S. Forrest, Adv. Mater. 14 (2002) 147.
[2] B. D'Andrade, S. Forrest, Adv. Mater. 16 (2004) 1585.
[3] C. Adachi, M.A. Baldo, M.E. Thompson, S.R. Forrest, J. Appl. Phys. 90 (2001) 5048.
[4] H. Sasabe, K. Minamoto, Y.-J. Pu, M. Hirasawa, J. Kido, Org. Electron. 13 (2012) 2615.
[5] G. Schwartz, S. Reineke, T.C. Rosenow, K. Walzer, K. Leo, Adv. Funct. Mater. 19 (2009) 1319.
[6] F. Zhao, Z. Zhang, Y. Liu, Y. Dai, J. Chen, D. Ma, Org. Electron. 13 (2012) 1049.
[7] M.C. Gather, A. Köhnen, K. Meerholz, Adv. Mater. 23 (2011) 233.
[8] W. Song, M. Meng, Y.H. Kim, C.B. Moon, C.G. Jhun, S.Y. Lee, R. Wood, W.Y. Kim, J. Lumin. 132 (2012) 2122.
[9] S.H. Yang, S.F. Huang, C.H. Chang, C.H. Chung, J. Lumin. 131 (2011) 2106.
[10] S.R. Forrest, D.D.C. Bradley, M.E. Thompson, Adv. Mater. 15 (2003) 1043.
[11] G. Xie, Z. Zhang, Q. Xue, S. Zhang, Y. Luo, L. Zhao, Q. Wu, P. Chen, B. Quan, Y. Zhao, S. Liu, J. Phys. Chem. C 115 (2010) 264.
[12] T. Zheng, W.C.H. Choy, Adv. Funct. Mater. 20 (2010) 648.
[13] Q. Xue, S. Zhang, G. Xie, Z. Zhang, Y. Luo, L. Zhao, P. Chen, Y. Zhao, S. Liu, Thin Solid Films 519 (2011) 3816.
[14] S. Zhang, G. Xie, Q. Xue, Z. Zhang, L. Zhao, Y. Luo, S. Yue, Y. Zhao, S. Liu, Thin Solid Films 520 (2012) 2966.
[15] J.-H. Jou, C.-J. Wang, Y.-P. Lin, Y.-C. Chung, P.-H. Chiang, M.-H. Wu, C.-P. Wang, C.-L. Lai, C. Chang, Appl. Phys. Lett. 92 (2008) 223504.
[16] P. Chen, Q. Xue, W. Xie, Y. Duan, G. Xie, Y. Zhao, J. Hou, S. Liu, L. Zhang, B. Li, Appl. Phys. Lett. 93 (2008) 153508.
[17] Z. Zhang, G. Xie, S. Yue, Q. Wu, Y. Chen, S. Zhang, L. Zhao, Y. Luo, Y. Zhao, S. Liu, Org. Electron. 13 (2012) 2296.
[18] R. Lin, F. Wang, J. Rybicki, M. Wohlgenannt, K.A. Hutchinson, Phys. Rev. B 81 (2010) 195214.
[19] M.-T. Lee, H.-H. Chen, C.-H. Liao, C.-H. Tsai, C.H. Chen, Appl. Phys. Lett. 85 (2004) 3301.
[20] G. He, M. Pfeiffer, K. Leo, M. Hofmann, J. Birnstock, R. Pudzich, J. Salbeck, Appl. Phys. Lett. 85 (2004) 3911.
[21] S. Reineke, F. Lindner, G. Schwartz, N. Seidler, K. Walzer, B. Lussem, K. Leo, Nature 459 (2009) 234.